

# Schrock Catalyst Triggered, Ring-Opening Metathesis Polymerization Based Synthesis of Functional Monolithic Materials

Bettina Scheibitz,<sup>†</sup> Andrea Prager,<sup>†</sup> and Michael R. Buchmeiser<sup>\*,†,‡</sup>

Leibniz-Institut für Oberflächenmodifizierung e.V., Permoserstrasse 15, D-04318 Leipzig, Germany, and Institut für Technische Chemie, Universität Leipzig, Linnéstrasse 3, D-04103 Leipzig, Germany

Received February 4, 2009; Revised Manuscript Received March 12, 2009

**ABSTRACT:** The synthesis of monolithic materials via the Schrock catalyst triggered ring-opening metathesis polymerization (ROMP) is described.  $\text{Mo}(\text{N}-2,6-(2\text{-Pr})_2\text{-C}_6\text{H}_3)(\text{CHCMe}_2\text{Ph})(\text{OCMe}_3)_2$  (**1**) was used as an initiator. Using various ratios of norborn-2-ene (NBE) and 1,4,4a,5,8,8a-hexahydro-1,4,5,8-*exo,endo*-dimethanonaphthalene (DMN-H6) in different mixtures of micro- with macroporogens, i.e., 1,2-dichloroethane, toluene and THF with hexane or pentane, monolithic polymeric materials with continuous, interconnected pores in the micrometer range as well as with micro- and mesopores in the 1.5–300 nm range could be synthesized within the confines of  $3 \times 100$  mm glass columns. The resulting monoliths were characterized via inverse size exclusion chromatography (ISEC) in terms of the total pore volume ( $V_p$ ), the volume fraction of the pore porosity ( $\epsilon_p$ ), the volume fraction of the interstitial porosity ( $\epsilon_z$ ) and the pore size distribution. Finally, the novel monoliths were successfully used for the fast separation of proteins as well as of 9-fluorenylmethoxycarbonyl (Fmoc) protected amino acids.

## Introduction

Monolithic polymeric materials as they are utilized today have first been reported in the early 1990s<sup>1–3</sup> and have nowadays become an integral part of polymer chemistry and material science. Originally designed for high-speed chromatographic separations, they are now also used for other applications, e.g., as catalytic supports in bioreactors.<sup>4</sup> Monolithic polymeric materials are characterized by a unitary porous structure with interconnected large pores and are usually synthesized within the confines of the compartment in which they are to be used at a later stage. This avoids any packing procedures. The structure-forming matrix, composed of interlinked microglobules, itself may be nonporous or porous, depending on the application. Particularly monoliths based on nonporous structure-forming microglobules allow for the separation of medium and high molecular weight analytes such as proteins, peptides, and oligonucleotides within very short times of analysis, typically within less than 60 s.<sup>5</sup> This is related to the fact that there is no diffusion of analytes into small pores. Instead, the entire interaction of the analytes with the stationary phase occurs at the nonporous inner surface of the monolith, giving resulting in fast mass transfer between the stationary and mobile phase.

So far, the majority of monolithic polymeric materials are prepared via thermally or UV-induced free radical polymerization of (meth)acrylates,<sup>5,6</sup> however, other techniques such as  $\gamma$ -irradiation<sup>7</sup> or electron beam triggered free radical polymerization<sup>8–12</sup> as well as various polyaddition and polycondensation based approaches have to be mentioned, too.<sup>13–15</sup> Apart from these synthetic approaches, the ring-opening metathesis polymerization (ROMP) based synthesis and functionalization of such supports has been elaborated by our group<sup>16,17</sup> aiming at applications in separation science,<sup>9,12,18–26</sup> heterogeneous catalysis<sup>27–32</sup> and tissue engineering.<sup>33</sup> So far, the synthetic protocol has been exclusively based on first- and second-generation Grubbs-type initiators, respectively. Here, we report on the first synthesis of monolithic polymeric supports via a Schrock catalyst-based synthetic protocol suitable for chromatographic separations.

## Results and Discussion

**Polymerization Kinetics.** Based on our results obtained with polymeric monoliths obtained from norborn-2-ene (NBE), 1,4,4a,5,8,8a-hexahydro-1,4,5,8-*exo,endo*-dimethanonaphthalene (DMN-H6), and the first-generation Grubbs catalyst,  $\text{RuCl}_2(\text{PCy}_3)_2(\text{CHPh})$ , we chose NBE and DMN-H6 for the present study. For the successful realization of a monolithic polymeric structure from NBE and DMN-H6, the rate constants of polymerization of both compounds need to be at least comparable with a given initiator; i.e., they should be within the same order of magnitude. Otherwise, block-type copolymers rather than random copolymers are obtained. We therefore investigated the polymerization kinetics of both NBE and DMN-H6 with  $\text{Mo}(\text{N}-2,6-(2\text{-Pr})_2\text{-C}_6\text{H}_3)(\text{CHCMe}_2\text{Ph})(\text{OCMe}_3)_2$  (**1**) in both homo- and in copolymerization. Due to the high activity of **1**, these polymerizations were carried out at  $-35^\circ\text{C}$ . The results are summarized in Table 1. The rate constants of polymerization at  $T = 25^\circ\text{C}$  were extrapolated from the values obtained at  $-35^\circ\text{C}$  assuming that  $k_p$  roughly doubles per  $10^\circ\text{C}$  increase in temperature. The kinetic plots as well as the first-order kinetic plots for NBE and DMN-H6 are shown in Figures 1 and 2.

As can be deduced therefrom, quantitative monomer conversion was achieved in less than 25 min for NBE and DMN-H6 in both homo- and copolymerization. In all cases, a linear plot of  $-\ln(c_{\text{monomer}})$  vs time was observed, indicative for first-order kinetics and quantitative initiation. As outlined earlier, such a living polymerization setup is of utmost importance for the reproducibility of synthesis and a unique feature of ROMP-derived monoliths.<sup>6,16,17,19,24,34</sup> In homopolymerization, the  $k_p(\text{NBE})$  is larger than, yet comparable to  $k_p(\text{DMN-H6})$ . In copolymerization, however,  $k_p$  of NBE decreases and the  $k_p$  for DMN-H6 increases. These observed changes in polymerization kinetics for both NBE and DMN-H6 in copolymerization compared to

**Table 1. Summary of Rate Constants of Polymerization ( $k_p$ ) for the Homo- and Copolymerization of NBE and DMN-H6<sup>a</sup>**

compound	$k_p$ ( $-35^\circ\text{C}$ )		$k_p$ ( $25^\circ\text{C}$ )	
	homopolym	copolym	homopolym	copolym
NBE	$5.0 \times 10^{-3}$	$2.0 \times 10^{-3}$	0.32	0.13
DMN-H6	$1.4 \times 10^{-3}$	$3.2 \times 10^{-3}$	0.086	0.21

<sup>a</sup> Initiator **1** was used throughout.

\* Corresponding author. E-mail: michael.buchmeiser@iom-leipzig.de

<sup>†</sup> Leibniz-Institut für Oberflächenmodifizierung e.V.

<sup>‡</sup> Institut für Technische Chemie, Universität Leipzig.

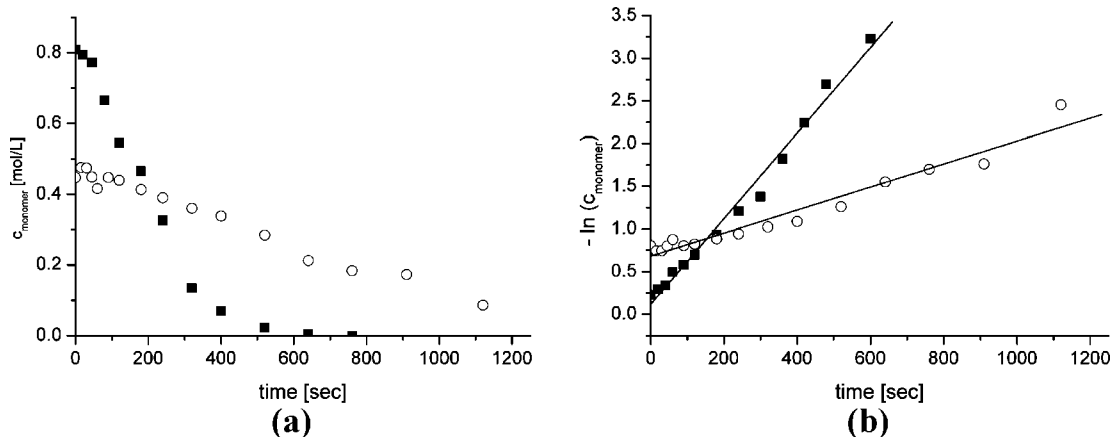


**Figure 1.** (a) Polymerization kinetics in the homopolymerization of NBE and DMN-H6, respectively, using **1** as initiator. (b)  $-\ln(c_{\text{monomer}})$  vs time for NBE and DMN-H6 homopolymerization. Key: (■) NBE; (○) DMN-H6.

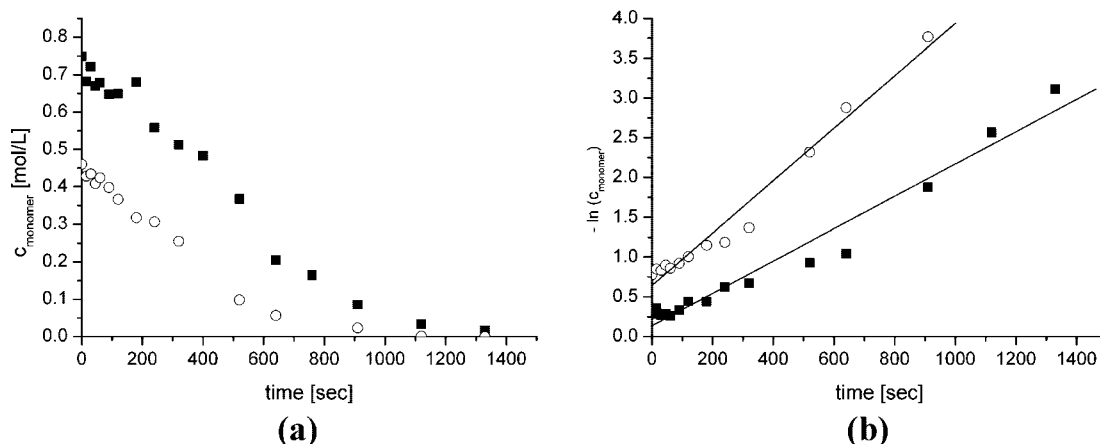


**Figure 2.** (a) Polymerization kinetics in the copolymerization of NBE with DMN-H6 using **1** as initiator. (b)  $-\ln(c_{\text{monomer}})$  vs time for the copolymerization of NBE with DMN-H6. Key: (■) NBE; (○) DMN-H6.

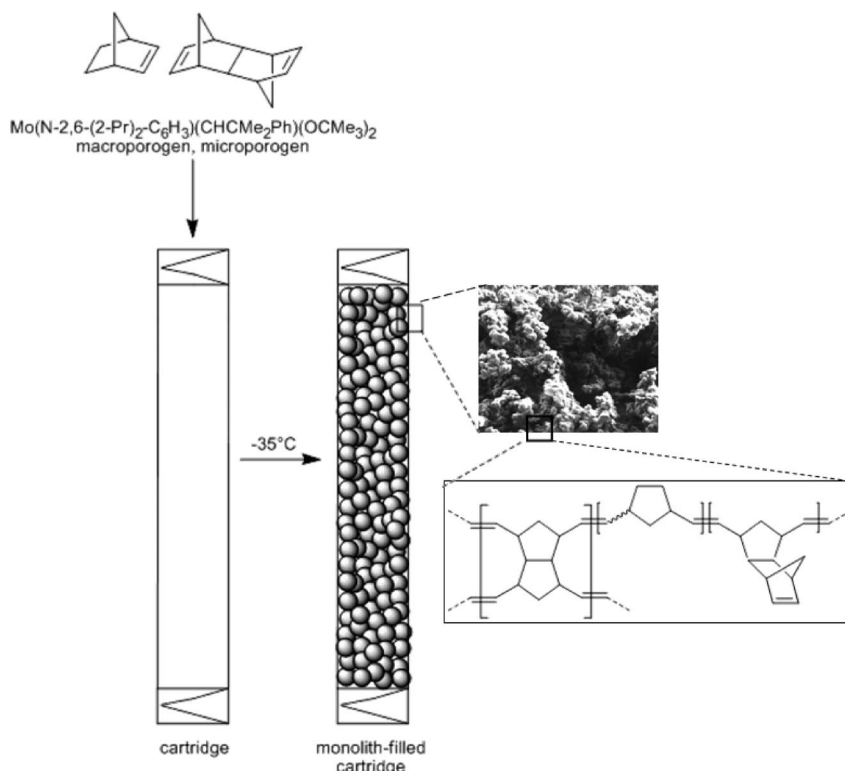
homopolymerization are attributed to a situation where the overall reactivity in copolymerization is mostly governed by DMN-H6. It is a sterically demanding, but due to its tricyclic nature, still a highly reactive compound. Its larger size as compared to NBE apparently disfavors consecutive insertions of DMN-H6 into the growing polymer chain in favor of DMN-H6 insertions followed by at least one NBE insertion. Since the  $k_p$  values for both monomers are very similar, one might well expect a highly alternating incorporation of both monomers into the growing polymer chain, depending on the stoichiometry between NBE and DMH-H6. Finally, it has to be stated that despite the virtually quantitative consumption of DMN-H6 during monolith synthesis, no statements on the degree of cross-linking can be made since ROMP preserves the double bond of the monomer.

**Polymerization System.** In order to obtain monoliths within the definitions of such materials (*vide supra*), a polymerization setup has to be created in which phase separation of an increasingly cross-linked matrix from the polymerization medium, usually consisting of a good and a poor polymer solvent serving as the micro- and macroporogen, is faster than gelation. According to the Flory–Huggins theory,<sup>35–37</sup> large, positive interaction parameters between the polymer and the solvent or solvent mixture are required in order to induce phase separation. Since norborn-2-ene (NBE) and 1,4,4a,5,8,8a-hexahydro-1,4,5,8-*exo,endo*-dimethanonaphthalene (DMN-H6) were used for monolith synthesis, at least one nonsolvent for both poly(NBE) and poly(DMN-H6) and thus also for poly(NBE)-*co*-poly(DMH-H6) had to be used. Only this way, phase separation can be

induced. While Grubbs-catalyst based ROMP protocols allow for the use of alcohols, most preferably of 2-propanol,<sup>16–31</sup> the reduced tolerance of Schrock catalysts versus protic compounds requires a different choice. We therefore investigated alternative macroporogens and found both pentane and the higher boiling hexane suitable for these purposes. While toluene is generally the preferred microporogen used in Grubbs catalyst-based protocols,<sup>16–31</sup> we additionally found 1,2-dichloroethane and THF suitable for use in combination with a Schrock catalyst. The final polymerization systems thus consisted of NBE, DMN-H6, a microporogen, e.g., 1,2-dichloroethane, toluene or THF, and a macroporogen, i.e. hexane or pentane, as well as of the initiator, i.e.  $\text{Mo}(\text{N}-2,6-(2\text{-Pr})_2\text{C}_6\text{H}_3)(\text{CHCMe}_2\text{Ph})(\text{OCMe}_3)_2$  (**1**) (Scheme 1, Table 2).

Though the Schrock catalyst used here is considered to be one with low activity compared to other Schrock catalysts, the polymerization mixture had to be prepared at  $-35^\circ\text{C}$  in order to avoid any uncontrolled polymerization. It was then filled into the surface-silanized columns and allowed to warm to room temperature. This way, monolith formation was virtually complete within minutes, however, reactions were allowed to proceed for 2 h. The catalyst was terminated by passing a 3 wt % solution of ferrocene carbaldehyde in THF through the monolith (flow rate 3 mL/min, 30 min) and the final monolith was extensively washed with THF in order to remove any monomeric or oligomeric byproducts. This simple Wittig-type reaction between the living polymer chains and an aldehyde does not only remove the initiator, but also provides a very simple and elegant way for in situ functionalization (Scheme

Scheme 1. Monolith Synthesis

Table 2. Selected Polymeric Monoliths Prepared from NBE and DMN-H6 and Different Micro- and Macroporogens<sup>b</sup>

monolith	NBE <sup>a</sup>	DMN-H6 <sup>a</sup>	macroporogen		microporogen		1 <sup>a</sup>
			pentane <sup>a</sup>	hexane <sup>a</sup>	toluene <sup>a</sup>	THF <sup>a</sup>	
1	20	20	50			10	0.2
2	20	20	50		10		0.2
3	20	20		50	10		0.2
4	20	20		50		10	0.2
5	10	10		70	10		0.1
6	20	20		55	5		0.2
7	15	15		65	5		0.1
8	10	30		50	10		0.1
9	10	20		60	10		0.1
10	0	40		50	10		0.1
11	5	35		50	10		0.1

monolith	NBE <sup>a</sup>	DMN-H6 <sup>a</sup>	hexane <sup>a</sup>	1,2-dichloroethane <sup>a</sup>	1 <sup>a</sup>
12	20	20	50	10	0.1
13	15	15	60	10	0.1

<sup>a</sup> wt %. <sup>b</sup> Initiator 1 was used throughout.

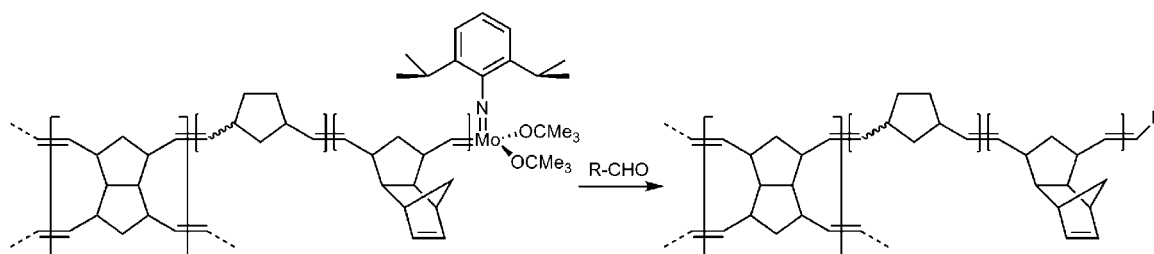
2). Thus, the nature of the functional group is basically only limited by the functionality of the corresponding aldehyde.

At this point it is worth mentioning that monomer conversion was unprecedentedly high. Thus, no remaining NBE or DMN-H6 could be determined by GC-MS at all, suggesting that

monomer conversion for both NBE and DMN-H6 was  $\gg 99.99\%$ . This illustrates the high reactivity and persistence of the Schrock catalyst during monolith synthesis. Inductively coupled optical emission spectrometry (ICP-OES) measurements on the final monolith revealed an Fe-content of 370 ppm, corresponding to  $6.6 \mu\text{mol/g}$  monolith. Since the amount of catalyst 1 used for monolith synthesis was  $6.1 \mu\text{mol/g}$  monomers, this results in a ratio of Fe:Mo of 1.08 ( $\sim 1$  within experimental error) and clearly illustrates both the quantitative initiation efficiency and the living character of the entire polymerization. Thus, the ratio of Fe:Mo can only equal 1 in case initiation was quantitative and a perfectly living system had been created. Only in this case, every living polymer chain is terminated by an aldehyde.

**Structural Characterization of Monoliths.** Table 2 summarizes a selection of recipes, i.e., different ratios of NBE:DMN-H6:macroporogen:microporogen:initiator that all lead to phase separation and the formation of polymeric monoliths. Toluene, THF and 1,2-dichloroethane have been successfully applied as microporogens. Both hexane and pentane may be used as macroporogens, however, hexane was preferably used because of its higher boiling point. This avoids the formation of gas bubbles generated by hot spots. The initiator was used on either a 0.1 or 0.2 wt % base. Figure 3 illustrates the different structures that were obtained. The resulting monoliths were then checked

Scheme 2. In Situ Functionalization of Polymeric Monoliths





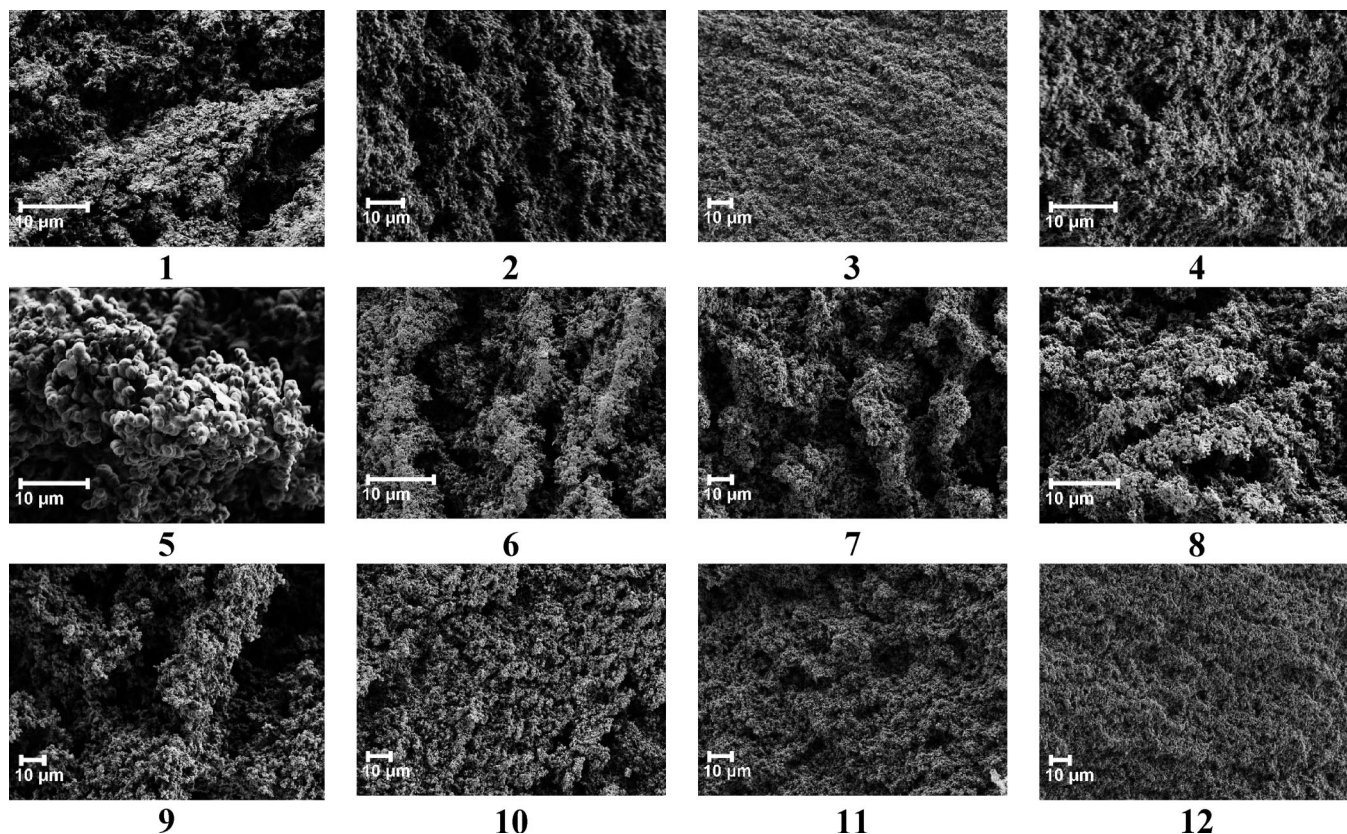


Figure 3. Transmission electron micrographs of monoliths 1–12.

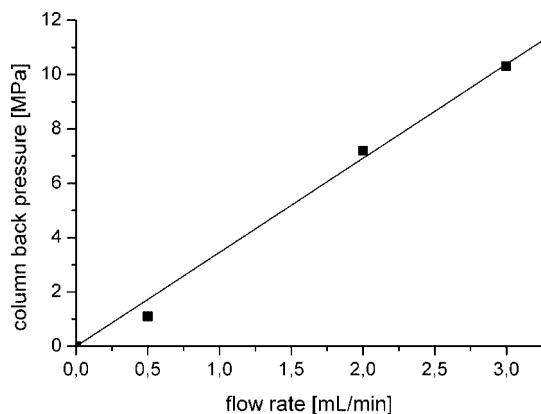


Figure 4. Graph of flow rate vs back pressure for monolith 13 (mobile phase: 95 wt % water, 5 wt % acetonitrile, 0.01 wt % TFA).

in terms of back pressure and pore size distribution. Typical flow rates that could be applied were  $\geq 3 \text{ mL} \cdot \text{min}^{-1}$ . Generally, a linear increase of back pressure vs. flow rate was observed. A typical graph of flow rate vs back pressure is shown in Figure 4.

From the different monoliths prepared by applying various recipes (Table 2), we identified a monolith that was expected and in fact turned out to be suitable for chromatographic separations. Thus, using a ratio of NBE:DMN-H6:1,2-dichloroethane:hexane:initiator of 15:15:10:60:0.1 (monolith 13, Table 2), a monolith with a total pore volume ( $V_p$ ) of  $145 \mu\text{L/g}$ , a volume fraction of pores ( $\epsilon_p$ ) of 21%, a volume fraction of intermicroglobule void volume ( $\epsilon_z$ ) of 68% and a mean microglobule diameter of  $0.4 \mu\text{m}$  was obtained. A scanning electron microscope image of this material is shown in Figure 5, the pore size distribution as determined by ISEC is shown in Figure 6.

As can be deduced from Figure 5, large interpenetrating pores approximately  $2\text{--}4 \mu\text{m}$  in diameter, which guarantee for a sufficient flow through the material, are visible. Figure 6 shows a comparable homogeneous pore size distribution between 30 and  $3000 \text{ \AA}$  and with a large fraction of pores (approximately 43%) in the 2 nm region.

**Chromatographic Separations.** A major advantage of monolithic materials is their ability to separate high molecular weight compounds within comparably short times. We used monolith 13 (Table 2) for the separation of 5 different proteins, i.e., ribonuclease A, lysozyme, albumin, insulin, and cytochrome c. As can be seen (Figure 7), these compounds were separated within less than 2.5 min using gradient elution based on a water/acetonitrile/trifluoroacetic acid based mobile phase. Peak widths at half-height ( $\omega_{1/2}$ ) were in the range of 1.3–3.1 s, resolution ( $R$ ) was between 1.61 and 1.88 (Table 3). Since the hydrodynamic radii of all analytes are  $>100 \text{ \AA}$ , the pores in the range between  $1 < \log(\Phi) < 2$  hardly participate in the separation process.

However, in view of the large volume fraction of very small pores (approximately 2 nm in size) of the monolithic material (Figure 5), we also anticipated a good separation capability of the novel monolithic stationary phases for small analytes, i.e., fluorenylmethoxycarbonyl (Fmoc) protected amino acids. A representative separation is shown in Figure 8.

In fact, the separation of Fmoc-glycine, Fmoc-L-alanine, Fmoc-L-proline, Fmoc-L-methionine, Fmoc-L-isoleucine, and Fmoc-L-phenylalanine was accomplished within less than 2 min, though with good resolution. Thus, peak widths at half-height were in the range of 1.9–5.5 s, resolution was between 1 and 2.6. Together with the capability of directly functionalizing the monolith, these two examples clearly underline the general potential of Schrock catalyst-derived monoliths.

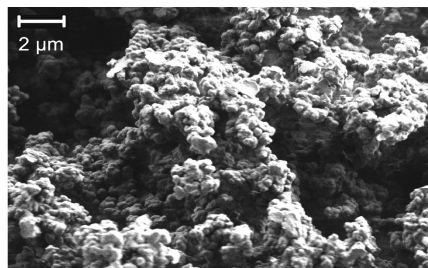


Figure 5. Electron micrographs of monolith 13.

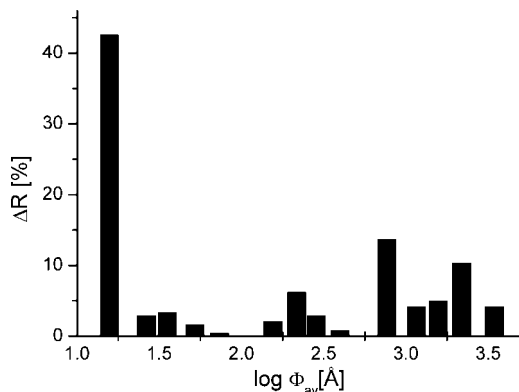


Figure 6. Graph of  $\Delta R$  (%) vs  $\log \Phi_{av}$  (Å) for monolith 13.

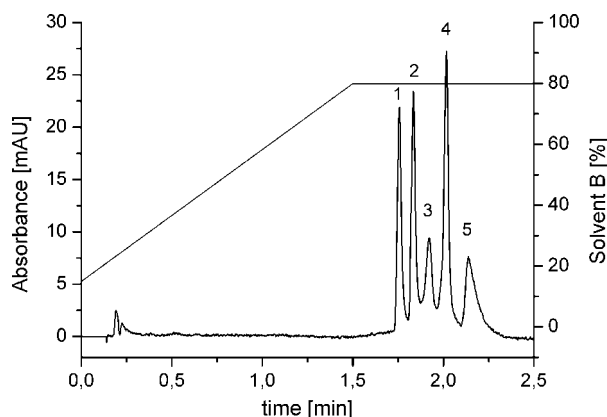


Figure 7. Separation of a protein standard on monolith 13. Peak order: (1) ribonuclease A, (2) insulin (3) cytochrome c, (4) lysozyme, (5) albumin. Chromatographic conditions. Mobile phase: (A) 95% water, 5% acetonitrile, 0.1% TFA; (B) 95% acetonitrile, 5% water, 0.1% TFA. Flow rate: 3 mL/min, 25 °C; UV (214 nm). Injection volume: 20  $\mu$ L (0.2  $\mu$ g). Gradient: 15–80% (B) within 1.5 min.

## Conclusions

The copolymerization of NBE with DMN-H6 in the presence of two nonprotic solvents, i.e., a polar (1,2-dichloroethane) and a nonpolar one (hexane) serving as macro- and microporogen, respectively, allows for the synthesis of monolithic media by the use of a Schrock catalyst. The resulting monolithic media are applicable to the separation of both low- and high-molecular weight analytes as illustrated by the separation of Fmoc-protected amino acids and various peptides. While the strength of synthetic protocols based on Grubbs-type initiators are related to the initiators' stability and tolerance versus water, oxygen and functional groups, Schrock catalyst-based protocols benefit from the high reactivity of the initiator and the ease of functionalization using aldehydes. Current work will address

Table 3. Summary of Retention Times ( $t_R$ ), Peak Widths at Half Height ( $w_{1/2}$ ) and Peak Resolution ( $R$ ) for Proteins and Fmoc-Protected Amino Acids

protein	$t_R$ [min]	$w_{1/2}$ [s]	$R$
ribonuclease A	1.76	1.4	1.61
insulin	1.83	1.3	1.77
cytochrome c	1.92	1.9	1.88
lysozyme	2.02	1.4	1.65
albumin	2.14	3.1	

Fmoc-amino acid	$t_R$ [min]	$w_{1/2}$ [s]	$R$
Fmoc-glycine	0.93	4.7	1.87
Fmoc-L-alanine	1.25	5.5	2.55
Fmoc-L-proline	1.63	4.1	2.12
Fmoc-L-methionine	1.82	2.0	1.53
Fmoc-L-isoleucine	1.90	1.9	1.01
Fmoc-L-phenylalanine	1.95	1.9	

the further functionalization of such supports and the results will be reported in due course.

## Experimental Section

**Chemicals and Reagents.** All manipulations were performed under a nitrogen atmosphere in an MBraun glovebox or by standard Schlenk techniques. Toluene, pyridine and THF were purchased from Merck (Darmstadt, Germany).  $Al_2O_3$  was purchased from Fluka (Seelze, Germany) and dried *in vacuo* at 180 °C for 24 h. 5-(Bicyclo[2.2.1]hept-2-en-5-yl)trichlorosilane was obtained from ABCR (Karlruhe, Germany). Narrow polystyrene (PS) standards with molecular masses ( $M_w$ ) of 440, 725, 1180, 2250, 4000, 6870, 17200, 23800, 42000, 75000, 301600, 400000, 803000, 1260000, and 3390000  $g \cdot mol^{-1}$  were purchased from Polymer Standards Service (PSS, Mainz, Germany). Norborn-2-ene, norbornadiene,

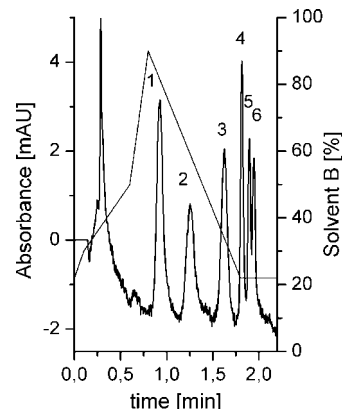


Figure 8. Separation of Fmoc-protected amino acids on monolith 13. Peak order. (1) Fmoc-glycine, (2) Fmoc-L-alanine, (3) Fmoc-L-proline, (4) Fmoc-L-methionine, (5) Fmoc-L-isoleucine, (6) Fmoc-L-phenylalanine. Chromatographic conditions. Mobile phase: (A) 100% water, 0.1% TFA; (B) 95% acetonitrile. Flow rate: 3 mL/min,  $T = 35$  °C; UV (214 nm). Injection volume was 1  $\mu$ L (0.01  $\mu$ g). Gradient: 22–30% (B) within 0.1 min, 30–50% (B) within 0.5 min, 50–90% (B) within 0.2 min.



1,2-dichloroethane, ribonuclease A (from bovine pancreas, 13700 g·mol<sup>-1</sup>), lysozyme (from chicken egg white, 14300 g·mol<sup>-1</sup>), albumin (from human serum, 66500 g·mol<sup>-1</sup>), insulin (from bovine pancreas, 5700 g·mol<sup>-1</sup>), cytochrome c (from bovine milk, 13000 g·mol<sup>-1</sup>), acetonitrile (HPLC gradient grade), water (HPLC grade), trifluoroacetic acid (TFA, 99.5%), *tert*-butylbenzene, and ferrocene carbaldehyde were obtained from Sigma–Aldrich (Seelze, Germany). 1,4,4a,5,8,8a-hexahydro-1,4,5,8-*exo,endo*-dimethanonaphthalene (DMN-H6) was prepared from freshly cracked cyclopentadiene and pure norbornadiene according to published procedures.<sup>38</sup> Mo(N-2,6-(2-Pr)<sub>2</sub>C<sub>6</sub>H<sub>3</sub>)(CHCMe<sub>2</sub>Ph)(OC(CH<sub>3</sub>)<sub>3</sub>)<sub>2</sub> (**1**) was prepared according to the literature.<sup>39,40</sup> ISEC measurements were carried out as described in ref.<sup>41</sup> Toluene, pentane and THF were dried by an MBraun SPS System (MBraun, Garching, Germany). Hexane was distilled from sodium/benzophenone. All solvents were passed over Al<sub>2</sub>O<sub>3</sub> prior to use. 1,2-Dichloroethane was distilled from CaH<sub>2</sub> and also passed over Al<sub>2</sub>O<sub>3</sub> prior to use. The protein standard was prepared by dissolving 1.0 mg of protein in 1.00 mL of peptide separation buffer. Prior to use, this standard was diluted in a 1:10 ratio in mobile phase A (cf. Figure 6). Fmoc-glycine, Fmoc-L-alanine, Fmoc-L-proline, Fmoc-L-methionine, Fmoc-L-isoleucine, and Fmoc-L-phenylalanine were purchased from Fluka (Seelze, Germany). The Fmoc-protected amino acid standard was prepared by dissolving 1.0 mg of each of the corresponding Fmoc-amino acid in 1.00 mL of pure acetonitrile. This standard was also diluted 1:10 prior to use.

**Instrumentation.** ICP-OES measurements were carried out on a Spectro ciros vision (Spectro Analytical Instruments GmbH&Co, Kleve, Germany). A microPREP 1500 (MLS-GmbH MIKROWELLEN-LABOR SYSTEME GmbH, Leutkirch, Germany) was used for microwave-assisted dissolution of the polymeric samples. A multielement standard containing Fe and Mo (1000 ppm, 1 N HNO<sub>3</sub>) was used. Standards for calibration (0–12 mg/L) were prepared there from. Fe-measurements were run at  $\lambda$  = 259.941 nm, the background was measured at  $\lambda$  = 259.77 and 260.03 nm, respectively. For inverse-size exclusion chromatography (ISEC), an L-4500 UV detector and an L-6200A HPLC pump (all Merck KGaA), equipped with a manual sample injection system was used. HPLC measurements were carried out on an HPLC system consisting of an SCL-10AVP system controller, an LC-10AT HPLC pump, an SIL-10A autoinjector, an SPD-M10AVP diode array detector, a CTO-10AC column oven and a CLASS-VP503 software (all by Shimadzu, Duisburg, Germany). Scanning electron microscopy (SEM) was carried out on a Carl Zeiss SMT Ultra 55 (Oberkochen, Germany).

**Characterization of Porous Properties.** Characterization was accomplished applying ISEC according to a published procedure.<sup>41</sup> For the measurements of retention times, 10  $\mu$ L samples of individual PS standards (1 mg/mL), dissolved in the mobile phase (THF), were injected onto the column applying a flow rate of 0.6 mL·min<sup>-1</sup>. For the determination of the total accessible porosity of the column, a 10  $\mu$ L sample of toluene was injected. All chromatograms were recorded at a wavelength of 254 nm. Retention times and volumes corresponding to each injection were determined from the peak maximum. Calculations were carried out assuming that the hydrodynamic radii of the PS standards in THF do not differ significantly from those reported in CH<sub>2</sub>Cl<sub>2</sub>.

**Synthesis of Monolithic Columns.** All experiments were carried out in a glovebox. All solvents were flushed through Al<sub>2</sub>O<sub>3</sub> prior to use in order to remove any residual water. Surface modified glass columns (3 mm  $\times$  100 mm) were prepared via etching of the columns with ethanolic KOH followed by silanization applying a mixture of toluene/pyridine/bicyclo[2.2.1]-hept-2-en-5-yltrichlorosilane (molar ratio 3.5:1.7:1) according to published procedures.<sup>18,42</sup> For monolith synthesis, two solutions were prepared. Solution A contained norborn-2-ene (NBE), 1,4,4a,5,8,8a-hexahydro-1,4,5,8-*exo,endo*-dimethanonaphthalene (DMN-H6) and the macroporogen. Solution B contained the microporogen and the initiator (**1**). Both solutions were cooled to -35 °C, mixed and rapidly transferred into the column. After 2 h, the column was taken out of the glovebox and flushed with THF containing 3 wt

% of ferrocene carbaldehyde (30 min, 3 mL/min), and then with THF.

**Polymerization Kinetics.** Two solutions were prepared. Solution A consisted of 1 mL of toluene, the monomer and *tert*-butylbenzene, which was used as an internal standard. Solution B consisted of 1 mL of toluene and the initiator. The two solutions were chilled to -35 °C, quickly mixed and samples were withdrawn in defined intervals. All polymerizations were terminated with ferrocene carbaldehyde, the samples were filtered and the monomers; i.e., NBE and DMN-H6 were quantified by GC-MS.

**Acknowledgment.** Our work was supported by a grant of the Deutsche Forschungsgemeinschaft (DFG, BU2174/1–2), the Federal Government of Germany, and the Freistaat Sachsen.

## References and Notes

- Tennikova, T. B.; Belenkii, B. G.; Švec, F. *J. Liq. Chrom. Relat. Technol.* **1990**, *13*, 63–70.
- Belenkii, B. G.; Podkladenko, A. M.; Kurenbin, O. I.; Mal'tsev, V. G.; Nasledov, D. G.; Trushin, S. A. *J. Chromatogr.* **1993**, *645*, 1–15.
- Mal'tsev, V. G.; Nasledov, D. G.; Trushin, S. A.; Tennikova, T. B.; Vinogradova, S. V.; Volokitina, I. N.; Zgonnik, V. N.; Belenkii, B. G. *J. High Resolut. Chromatogr.* **1990**, *13*, 185–189.
- Xie, S.; Švec, F.; Fréchet, J. M. J. *Biotechnol. Bioeng.* **1999**, *62*, 30–35.
- Švec, F.; Tennikova, T. B.; Deyl, Z. *Monolithic Materials: Preparation, Properties and Application. J. Chromatogr., Libr. Ed.* **2003**, *67*, 1–773.
- Buchmeiser, M. R. *Polymer* **2007**, *48*, 2187–2198.
- Sáfrány, A.; Beiler, B.; László, K.; Švec, F. *Polymer* **2005**, *46*, 2862–2871.
- Bandari, R.; Knolle, W.; Prager-Duschke, A.; Buchmeiser, M. R. *Macromol. Chem. Phys.* **2007**, *208*, 1428–1436.
- Bandari, R.; Knolle, W.; Buchmeiser, M. R. *Macromol. Rapid Commun.* **2007**, *28*, 2090–2094.
- Bandari, R.; Knolle, W.; Buchmeiser, M. R. *Macromol. Symp.* **2007**, *254*, 87–92.
- Bandari, R.; Elsner, C.; Knolle, W.; Kühnel, C.; Decker, U.; Buchmeiser, M. R. *J. Sep. Sci.* **2007**, *30*, 2821–2827.
- Bandari, R.; Knolle, W.; Buchmeiser, M. R. *J. Chromatogr. A* **2008**, *1191*, 268–273.
- Hosoya, K.; Hira, N.; Yamamoto, K.; Nishimura, M.; Tanaka, N. *Anal. Chem.* **2006**, *78*, 5729–5735.
- Tsujioaka, N.; Hira, N.; Aoki, S.; Tanaka, N.; Hosoya, K. *Macromolecules* **2005**, *38*, 9901–9903.
- Nguyen, A. M.; Irgum, K. *Chem. Mater.* **2006**, *18*, 6308–6315.
- Sinner, F.; Buchmeiser, M. R. *Angew. Chem.* **2000**, *112*, 1491–1494. *Angew. Chem. Int. Ed.* **2000**, *39*, 1433–1436.
- Sinner, F.; Buchmeiser, M. R. *Macromolecules* **2000**, *33*, 5777–5786.
- Mayr, B.; Tessadri, R.; Post, E.; Buchmeiser, M. R. *Anal. Chem.* **2001**, *73*, 4071–4078.
- Buchmeiser, M. R. *Macromol. Rapid Commun.* **2001**, *22*, 1081–1094.
- Lubbad, S.; Mayr, B.; Huber, C. G.; Buchmeiser, M. R. *J. Chromatogr. A* **2002**, *959*, 121–129.
- Lubbad, S.; Buchmeiser, M. R. *Macromol. Rapid Commun.* **2002**, *23*, 617–621.
- Gatschelhofer, C.; Magnes, C.; Pieber, T. R.; Buchmeiser, M. R.; Sinner, F. M. *J. Chromatogr. A* **2005**, *1090*, 81–89.
- Lubbad, S.; Steiner, S. A.; Fritz, J. S.; Buchmeiser, M. R. *J. Chromatogr. A* **2006**, *1109*, 86–91.
- Bandari, R.; Prager-Duschke, A.; Kühnel, C.; Decker, U.; Schlemmer, B.; Buchmeiser, M. R. *Macromolecules* **2006**, *39*, 5222–5229.
- Schlemmer, B.; Gatschelhofer, G.; Pieber, T. R.; Sinner, F. M.; Buchmeiser, M. R. *J. Chromatogr. A* **2006**, *1132*, 124–131.
- Sinner, F. M.; Gatschelhofer, C.; Mautner, A.; Magnes, C.; Buchmeiser, M. R.; Pieber, T. R. *J. Chromatogr. A* **2008**, *1191*, 274–281.
- Mayr, M.; Mayr, B.; Buchmeiser, M. R. *Angew. Chem.* **2001**, *113*, 3957–3960. *Angew. Chem. Int. Ed.* **2001**, *40*, 3839–3842.
- Buchmeiser, M. R.; Lubbad, S.; Mayr, M.; Wurst, K. *Inorg. Chim. Acta* **2003**, *345*, 145–153.
- Krause, J. O.; Lubbad, S.; Nuyken, O.; Buchmeiser, M. R. *Adv. Synth. Catal.* **2003**, *345*, 996–1004.
- Krause, J. O.; Lubbad, S. H.; Nuyken, O.; Buchmeiser, M. R. *Macromol. Rapid Commun.* **2003**, *24*, 875–878.
- Mayr, M.; Wang, D.; Kröll, R.; Schuler, N.; Prühs, S.; Fürstner, A.; Buchmeiser, M. R. *Adv. Synth. Catal.* **2005**, *347*, 484–492.
- Beier, M. J.; Knolle, W.; Prager-Duschke, A.; Buchmeiser, M. R. *Macromol. Rapid Commun.* **2008**, *29*, 904–908.

- (33) Löber, A.; Verch, A.; Schlemmer, B.; Höfer, S.; Frerich, B.; Buchmeiser, M. R. *Angew. Chem.* **2008**, *120*, 9279–9281. *Angew. Chem. Int. Ed.* **2008**, *47*, 9138–9141.
- (34) Buchmeiser, M. R. *J. Sep. Sci.* **2008**, *31*, 1907–1922.
- (35) Huggins, M. L. *J. Phys. Chem.* **1942**, *46*, 151–158.
- (36) Flory, P. J. *J. Chem. Phys.* **1942**, *10*, 51–61.
- (37) Huggins, M. L. *J. Am. Chem. Soc.* **1942**, *64*, 1712–1719.
- (38) Stille, J. K.; Frey, D. A. *J. Am. Chem. Soc.* **1959**, *81*, 4273.
- (39) Schrock, R. R.; Murdzek, J. S.; Bazan, G. C.; Robbins, J.; DiMare, M.; O'Regan, M. *J. Am. Chem. Soc.* **1990**, *112*, 3875–3886.
- (40) Oskam, J. H.; Fox, H. H.; Yap, K. B.; McConville, D. H.; O'Dell, R.; Lichtenstein, B. J.; Schrock, R. R. *J. Organomet. Chem.* **1993**, *459*, 185–197.
- (41) Halász, I.; Martin, K. *Angew. Chem.* **1978**, *90*, 954–961. Halász, I.; Martin, K. *Angew. Chem. Int. Ed.* **1978**, *17*, 901–909.
- (42) Mayr, B.; Buchmeiser, M. R. *J. Chromatogr. A* **2001**, *907*, 73–80.

MA9001963